Supplemental Materials

Molecular Biology of the Cell

Sawant et al.

Supplemental Figure 1

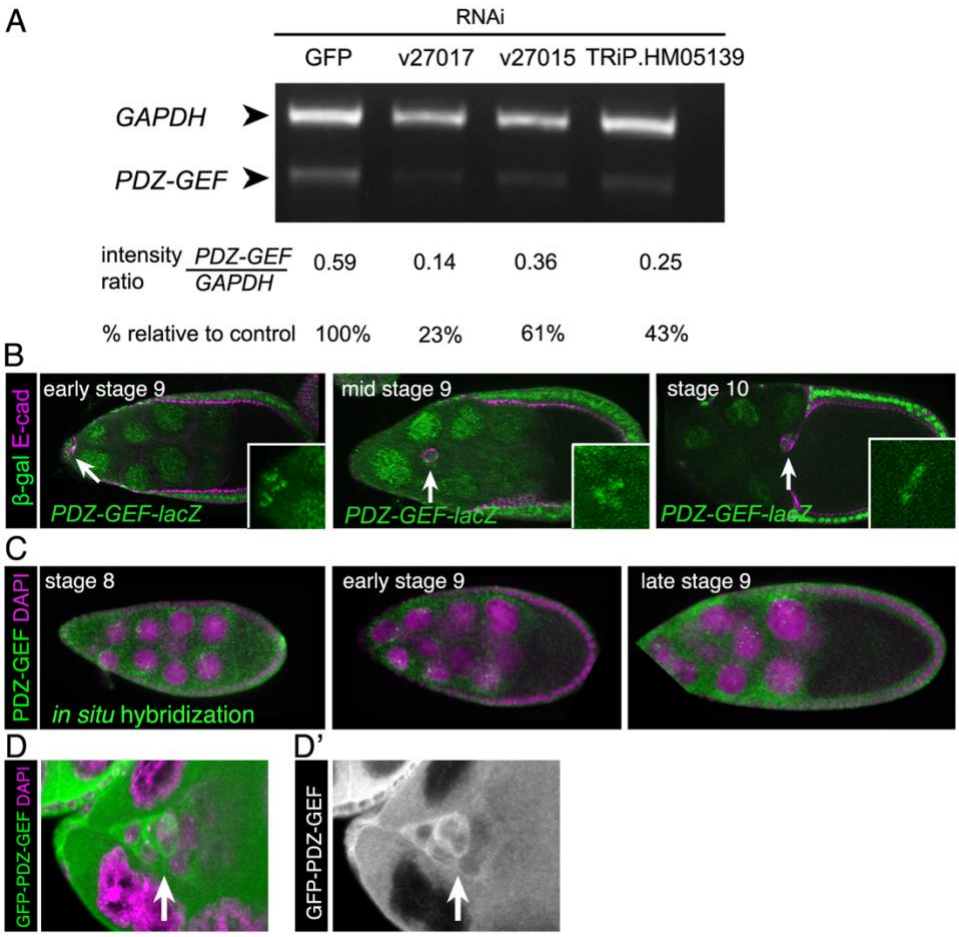

Supplemental Figure 1. Expression of *PDZ-GEF* and efficiency of *PDZ-GEF* knockdown by RNAi. (A) Effectiveness of RNAi was confirmed by performing RT-PCR on target mRNA from whole flies expressing GFP RNAi (control) or three different PDZ-GEF RNAi lines (v27017, v27015 and TRiP.HM05139). PCR products that amplified *PDZ-GEF* mRNA and *GAPDH* mRNA (loading control) were run on an agarose gel. Relative band intensities were measured and the ratios of *PDZ-GEF* to *GAPDH* were calculated. Percentage relative knockdown of *PDZ-GEF* was quantified compared to control (GFP RNAi). (B) Expression pattern of *PDZ-GEF-lacZ* during stages 9 and 10. Egg chambers expressing a *lacZ* enhancer trap in *PDZ-GEF* (*PDZ-GEF*^{1}/+) were stained for ß-galactosidase (ß-gal; green) and E-cadherin (E-cad; magenta) to mark cell membranes. *PDZ-GEF-lacZ* is expressed in all cells including the border cells (arrows). (C) In situ hybridization pattern of *PDZ-GEF* (CG9491) RNA in green at stages 8 and 9. Nuclear DNA stained for DAPI is shown in magenta. Open sourced images and data are from http://tomancak-srv1.mpi-cbg.de/DOT/main (Dresden Ovary Table: insitu56784, insitu56787, insitu56788; probe from RH54455 cDNA) (Jambor *et al.*, 2015). (D and D') Ubiquitous expression pattern of GFP-PDZ-GEF. Close-up view of an early stage 9 border cell cluster (arrow) expressing the GFP-PDZ-GEF genomic rescue construct (anti-GFP antibody; green in D; white in D') (Boettner and Van Aelst, 2007). DAPI (magenta) labels nuclear DNA in all cells.

Supplemental Figure 2

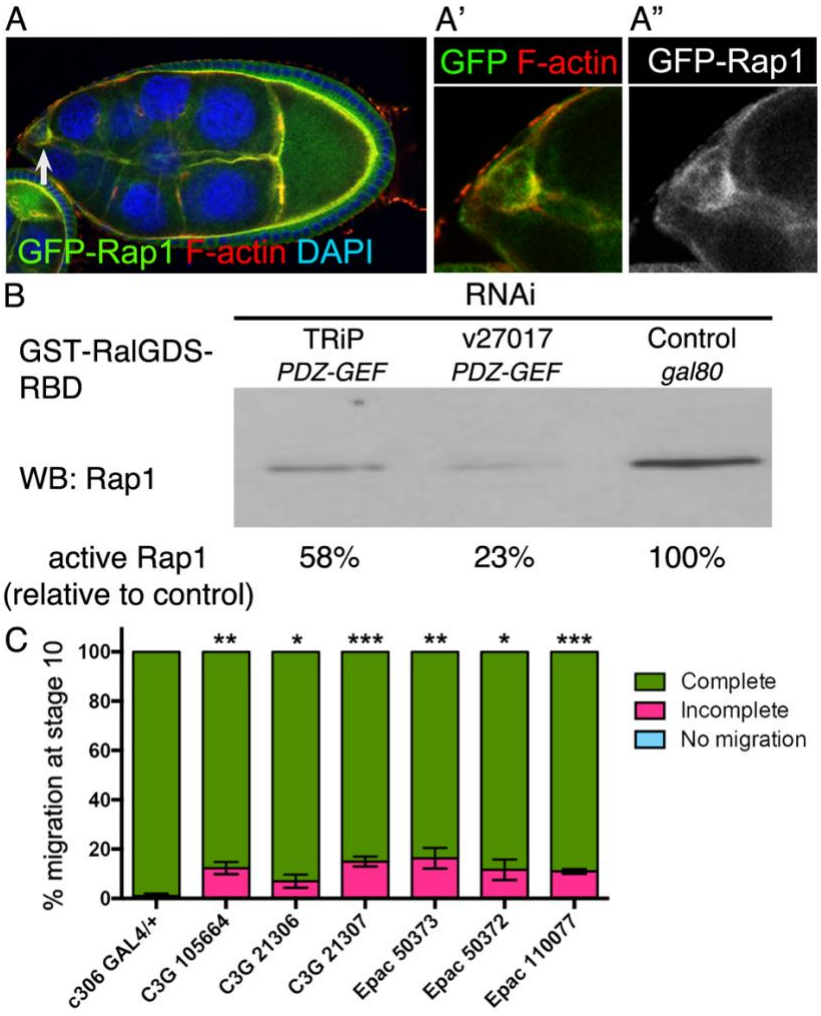

Supplemental Figure 2. Rap1 expression in early border cells and regulation by GEFs. (A-A") Stage 9 egg chamber during detachment stage expressing GFP-Rap1 (green in A and A'; white in A"), co-stained for DAPI (blue in A) to label nuclear DNA and phalloidin to label F-actin (red; A and A'). (A' and A'') Magnified view of the border cell cluster in A. Arrow (A) points to border cells. (B) Independent repeat of Rap1 activity pull-down assay on cell extracts from S2 cells treated with double-stranded RNA (RNAi) for PDZ-GEF (v27107 and TRiP.HM05139 RNAi) and *gal80* (control RNAi); see Figure 2C and Materials and Methods for further details. Relative band intensities were measured as a percentage of the control, which represents the maximum active Rap1 in this assay. (C) Quantification of complete (green), incomplete (pink), and no (blue) migration in stage 10 control (*c306*-GAL4/+) and UAS-C3G RNAi or UAS-Epac RNAi (*c306*-GAL4/+; +/UAS-RNAi). The numbers refer to the UAS-RNAi line number (see Materials and Methods for details). Values consist of four trials, with each trial assaying n ≥ 50 egg chambers (total n ≥ 153 egg chambers per genotype); *, $p < 0.05$; **, $p < 0.01$; ***, $p < 0.001$; unpaired two-tailed *t* test, comparing "complete" migration between control and RNAi lines. Error bars: ± SEM.

Supplemental Figure 3

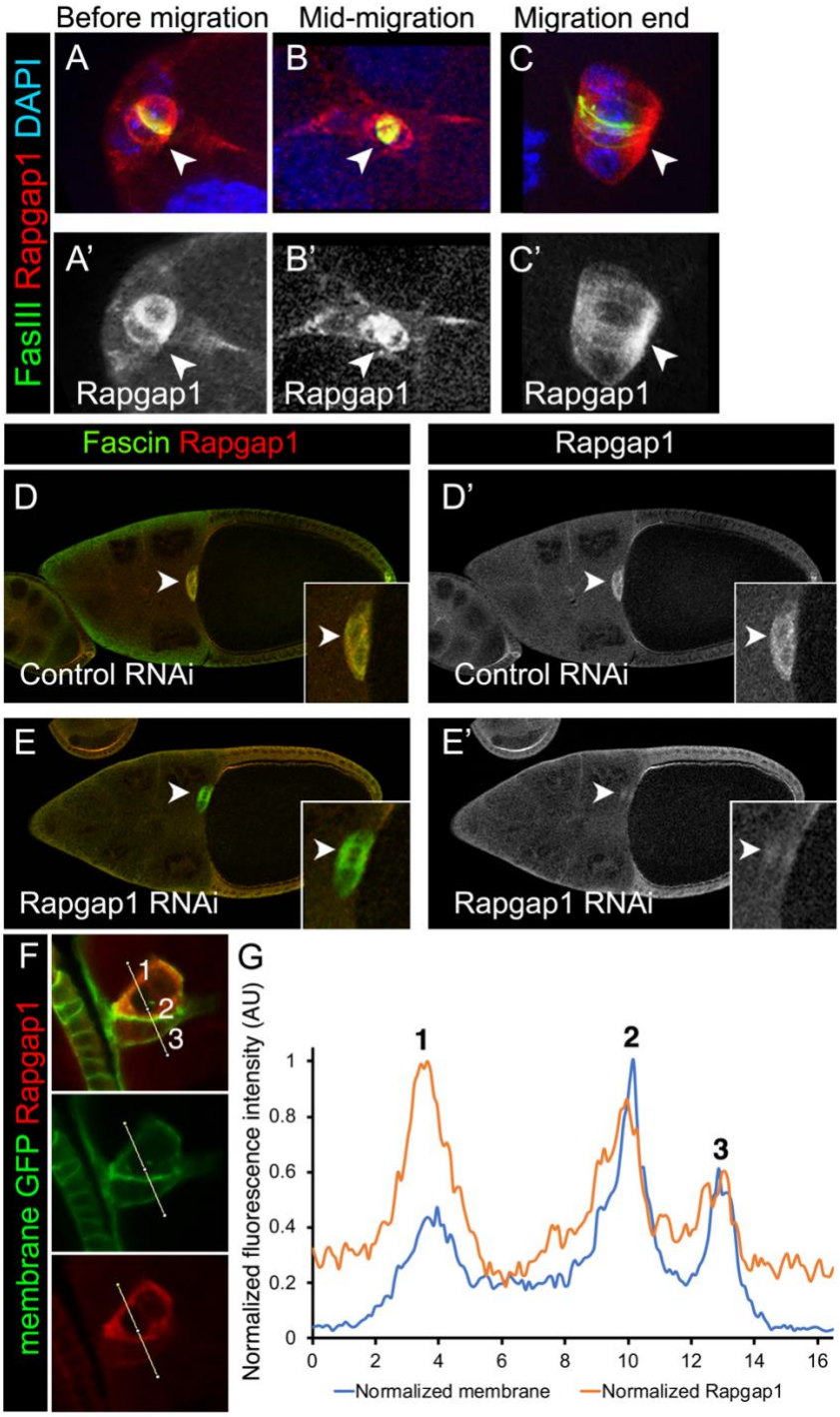

Supplemental Figure 3. Efficiency of Rapgap1 RNAi and Rapgap1 protein expression in polar cells within the border cell cluster. (A-C') Rapgap1 is expressed at high levels in the central polar cells (arrowheads). Stage 9 and 10 egg chambers co-stained for Rapgap1 (red in A-C; white in A'-C') and the polar cell marker Fasciclin III (FasIII; green; colocalization appears as yellow in A-C). FasIII accumulates at the membrane interface between polar cells (Ruohola *et al.*, 1991). (A-B') During the start of migration and during mid-migration, polar cells express high

levels of both Rapgap1 and FasIII; border cells express relatively lower levels of Rapgap1. (C and C') By the end of migration, equally high levels of Rapgap1 are detected in polar cells and border cells. (D-E') Stage 10 control (*slbo*-GAL4/UAS-mCherry RNAi) and Rapgap1 RNAi (*slbo*-GAL4/+; +/UAS-Rapgap1 RNAi) egg chambers were stained for Fascin (green) to label border cells and polar cells and for Rapgap1 (red). Insets, magnified views of the same border cell clusters. (D and D') control border cells and polar cells (arrowheads) have high levels of Rapgap1. (E and E') Rapgap1 RNAi border cells have severely reduced Rapgap1 protein levels; the polar cells (arrowheads) still express Rapgap1 because *slbo*-GAL4 is expressed in border cells but not polar cells (Geisbrecht and Montell, 2002). In the example shown, Rapgap1 RNAi border cells completed their migration; in ~15% of egg chambers, the border cells stopped along the migration pathway (see Figure 4I). (F and G) A subset of Rapgap1 protein is membrane-associated. (F) Single slice of a *z*-confocal stack of a border cell cluster that expresses membrane GFP (green; *c306*-GAL4/+; UAS-PLCΔPH-GFP/+) and is co-stained for anti-Rapgap1 (red). A "plot profile" (yellow line) was drawn in FIJI and used to measure relative fluorescence intensity of membrane GFP and Rapgap1 across polar cells (1 and 2) and border cells (3). (G) Plot of normalized membrane GFP (blue) and Rapgap1 (orange line) fluorescence pixel intensity (AU, arbitrary units) across the line shown in F, with numbers referring to the positions along the line. Plot regions to the left of (1) and right of (3) represent fluorescence intensity of adjacent nurse cells. Similar results were obtained from additional border cell clusters (n = 7).

Supplemental Figure 4

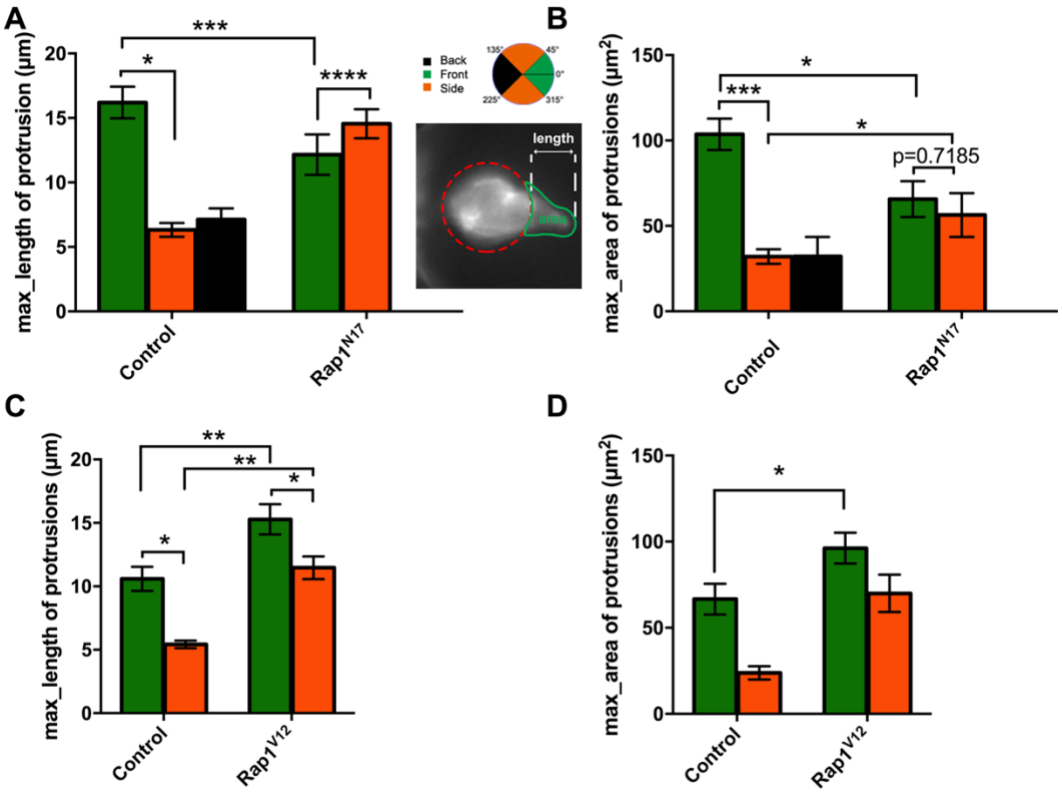

Supplemental Figure 4. Rap1 regulates the maximal protrusion length and area. Quantification of the maximum length (A and C) and maximum area (B and D) of protrusions from time-lapse movies of the indicated genotypes. Protrusions at the front (green), side (orange) and back (black) of control and Rap1 mutant border cell clusters were measured. (Inset, A) Close-up view of a live border cell cluster showing how the main body of the border cell cluster (orange line), protrusion length (white line) and protrusion area (green outlined area) were defined and measured. In this example the protrusion is at the "front" (green) and not at the "side" (orange). (A) $Rap1^{N17}$ border cells have shorter front protrusions and longer side protrusions compared to control. (B) The maximum area of $Rap1^{N17}$ front border cell protrusions is reduced, but is increased for side protrusions, compared to control. (C) $Rap1^{V12}$ border cells have longer front and side protrusions compared to control. (D) The maximum area of $Rap1^{V12}$ border cell protrusions, especially at the front, is increased compare to control. Genotypes in A and B: *c306*-GAL4, tsGAL80/+; +/*slbo*-LifeAct-GFP (control) and *c306*-GAL4, tsGAL80/+; UAS-$Rap1^{N17}$/*slbo*-LifeAct-GFP ($Rap1^{N17}$); genotypes in C and D: *slbo*-GAL4/*slbo*-LifeAct-GFP (control) and *slbo*-GAL4/*slbo*-LifeAct-GFP; UAS-$Rap1^{V12}$/+ ($Rap1^{V12}$). Values consist of protrusions measured from n ≥ 7 movies for each genotype (see Figure 5 for details); *, $p < 0.05$; **, $p < 0.01$; ***, $p < 0.001$; all other values were not significant ($p \geq 0.05$) and not shown (except in B); unpaired two-tailed *t* test. Error bars: SEM.

Supplemental References

Boettner, B., and Van Aelst, L. (2007). The Rap GTPase activator Drosophila PDZ-GEF regulates cell shape in epithelial migration and morphogenesis. Mol Cell Biol 27, 7966–7980.

Geisbrecht, E. R., and Montell, D. J. (2002). Myosin VI is required for E-cadherin-mediated border cell migration. Nat Cell Biol 4, 616–620.

Jambor, H., Surendranath, V., Kalinka, A. T., Mejstrik, P., Saalfeld, S., and Tomancak, P. (2015). Systematic imaging reveals features and changing localization of mRNAs in Drosophila development. eLife 4, R106.

Ruohola, H., Bremer, K. A., Baker, D., Swedlow, J. R., Jan, L. Y., and Jan, Y. N. (1991). Role of neurogenic genes in establishment of follicle cell fate and oocyte polarity during oogenesis in Drosophila. Cell 66, 433–449.